Algorithm Theoretical Basis Document of aerosol by non-polarization for GCOM-C/SGLI

2017.06 JAXA/EORC

Table of Contents

1. Introduction

Aerosols influence the energy budget of the earth’s climate system through scattering and absorbing solar radiation. For a more precise estimation of the impact of aerosols on climate systems, investigation of the behavior of aerosols on a global scale is essential but challenging because aerosol amounts and characteristics vary over space and time.

The multiple uses of various imaging sensors on both geostationary and polar-orbiting satellites are helpful to understand a complete picture of aerosol distribution in the global scale. The common algorithm for various sensors over different ground targets (ocean/land) provides more consistent aerosol retrievals over the globe than independent algorithms.

Therefore we developed a common retrieval algorithm of the aerosol optical properties to various satellite sensors based on the method developed by Higurashi and Nakajima (1998) and Fukuda et al. (2013). This approach was applied to GCOM-C/SGLI non-polarization channels. The SGLI channels used for the retrieval are given in section 2. The details of the retrieval methodology is explained in sections 3. Details on the candidate aerosol models and lookup table are described in sections 4 and 5, respectively.

2. Channels for aerosol retrieval by SGLI

The SGLI channels used for the aerosol retrieval are listed on Table 1. Only the channels longer than 800 nm are used for the algorithm over ocean, although all well-calibrated channels without strong gas absorption from visible to near-infrared wavelengths are used for the algorithm over land. The optimum channels for aerosol retrieval are automatically selected. Details of the automatic selection of the optimum channels are given in section 3.

Table 1 Channels of SGLI for aerosol retrieval

CH	center of wavelength[nm]	spatial resolution [m]	ocean	land
VN1	380	250		x
VN2	412			x
VN3	443			x
VN4	490			x
VN5	530			x
VN6	565			x
VN7	673.5			
VN8	673.5			x
VN9	763	1000		
VN10	868.5	250	x	
VN11	868.5			x
SW1	1050	1000	x	x
SW2	1380			
SW3	1630	250	x	x
SW4	2210	1000	x	x

3. Basic principles of the aerosol retrieval algorithm

We developed a common retrieval algorithm of the aerosol optical properties to various satellite sensors based on the method developed by Higurashi and Nakajima (1998) and Fukuda et al. (2013). Angstrom exponent (α) at 500 nm. First, we selected the clear-sky (i.e., cloud-free) pixel using a cloud detection algorithm developed for GCOM-C/SGLI (Ishida and Nakajima, 2009; Ishida et al. 2011). We then corrected the observed TOA reflectance at a channel *i* (ρ_{i}^{obs}) for gas absorption at visible to near-infrared regions. The gas correction was conducted for ozone and water vapor because their amounts vary significantly with time and location. The corrected TOA reflectance corresponding to US standard atmosphere ($\rho_{\mathrm{i}}^{obs\prime}$) is given by

$$\rho_{\mathrm{i}}^{obs\prime} = \frac{T_i^{O_3(USS)}}{T_i^{O_3(OMI)}} \cdot \frac{T_i^{H_2O(USS)}}{T_i^{H_2O(GGLA)}} \cdot \rho_{\mathrm{i}}^{obs}, \quad (1)$$

where $\mathrm{T_i^{O_3(OMI)}}$ and $T_i^{H_2O(GGLA)}$ are the transmission factors for ozone and water vapor at observation points, respectively, and $\mathrm{T_i^{O_3(USS)}}$ and $T_i^{H_2O(USS)}$are those for US standard atmosphere, respectively. We used the total ozone columns from Ozone Monitoring Instrument (OMI) on board the NASA EOS/Aura spacecraft (https://aura.gsfc.nasa.gov/omi.html) and column water vapor from JMA objective analysis data. The transmission factors $T_i^{O_3}$ and $T_i^{H_2O}$were preliminarily calculated for various total ozone columns (O) and column water vapor (w). Subsequently, the coefficients $K_i^{O_3}$, $K_{i,1}^{H_2O}$,$K_{i,2}^{H_2O}$, and $K_{i,3}^{H_2O}$ were derived from the fitting of Eqs. (2) and (3) based on MODIS Algorithm Theoretical Basis Document for Collection 005 and 051:

$$T_i^{O_3} = \exp(-GK^{O_3}O), \quad (2)$$

$$T_i^{H_2O} = \exp\left(-\exp\left(K_{i,1}^{H_2O} + K_{i,2}^{H_2O}\ln(Gw) + K_{i,2}^{H_2O}(\ln(Gw))^2\right)\right), \quad (3)$$

where the air mass factor (G) is a function of solar (θ_0) and sensor zenith angle (θ), such that

$$G = \frac{1}{\cos(\theta_0)} + \frac{1}{\cos(\theta)}. \quad (4)$$

We derived the optimum τ_a and the aerosol model (i.e., η and ω) from the candidate aerosol models given in section 2.1a, which minimize the object function J (Eq. 5) using $\rho_{\mathrm{i}}^{obs\prime}$ and the simulated TOA reflectance (ρ_{i}^{sim}) by a radiative transfer model:

$$J = \sum_i \left[w_i \cdot \left(\rho_i^{obs} - \rho_i^{sim}\right)^2\right] + \left(\frac{\partial \rho_k^{sim}}{\partial \omega}\right)^2 \cdot (\omega - \omega_a)^2, \quad (5)$$

where ω_a is a prior estimate of the single-scattering albedo at 500 nm, and w_i is the weight for each channel. In this study, w_i was calculated using Eq. (6):

$$w_i = \left(\frac{\partial \rho_i^{sim}}{\partial \tau_a}\right)^2 \cdot \frac{1}{\sigma_i^2}, \quad (6)$$

where σ_i is the uncertainty in the TOA reflectance. Given that σ_i mainly comes from sensor noise (σ_n) and uncertainty in the estimated target land/ocean-surface reflectance ($\Delta\rho_i^s$), we calculated σ_i from Eq. (7):

$$\sigma_i^2 = \sigma_s^2 + \sigma_n^2, \quad (7)$$

where σ_s is the uncertainty in the TOA reflectance resulting from $\Delta\rho_i^s$. We assumed $\Delta\rho_i^s$ to be 5% of surface reflectance (ρ_i^s), although we set $\Delta\rho_i^s$ to be 0.02 when the calculated $\Delta\rho_i^s$ was less than 0.02. We calculated σ_n from the signal-to-noise ratio at the sensor ground test. We selected the relatively accurate channels, whose TOA reflectance has smaller uncertainty, by giving larger weight to these channels. By considering $\frac{\partial\rho_i^{sim}}{\partial\tau_a}$ in Eq. (6), we also chose the channels at which the sensitivity of ρ_i^{sim} to τ_a was relatively large, that is, τ_a was estimated sensitively from the variation in ρ_i^{sim}. Considering that our algorithm was applied on various satellite sensors with different wavelengths, Eqs. (5)–(7) were designed to automatically select the optimum channels to estimate the aerosol parameters by considering w_i written in Eq. (6). We also added the second term in J (Eq. 5) to restrain ω in vicinity to ω_a, because the first term in J was minimized for various ω in case ρ_i^{sim} had less sensitivity to ω. ρ_k^{sim} in Eq. (5) was defined as the TOA reflectance at the channel *k*, which had the largest w_i, and ω_a was assumed to be 1 unless the observation for ω_a was utilized.

The TOA reflectance ρ_i^{sim} at a particular channel *i* can be approximated by

$$\rho_i^{sim}(\theta_0, \theta, \varphi) = \rho_i^a(\theta_0, \theta, \varphi) + \frac{t_i^s(\theta_0) \cdot t_i^v(\theta) \cdot \rho_i^s(\theta_0, \theta, \varphi)}{1 - s_i \cdot \rho_i^s(\theta_0, \theta, \varphi)}, \quad (8)$$

where ρ_i^a is the atmospheric path reflectance, and t_i^s and t_i^v represent total transmittance from the solar to the surface and from the surface to the sensor, respectively. s is the spherical albedo of the atmosphere, and ρ_i^s is the surface reflectance. These parameters are the functions of solar zenith angle (θ_0), satellite zenith angle (θ), and solar/satellite relative azimuth angles (φ). ρ_i^s was calculated based on the method by Fukuda et al. (2013), and we adopted the second lowest reflectance in a month because the lowest reflectance was occasionally interfered by cloud shadows. To reduce the effect of bidirectional characteristics of the surface, we used the surface reflectance at the same geometry for the determination of ρ_i^s. In the calculation of ρ_i^{sim} over ocean, we added the TOA reflectance resulting from direct sunlight reflected by the sea surface (sun glitter) to Eq. (8). The sea surface reflectance was calculated using observed wind speed based on the model by Cox and Munk (1954). Only the channels longer than 800 nm were used for the algorithm over ocean to avoid the influence of water-leaving radiance, although all well-calibrated channels from visible to near-infrared wavelengths were used for the algorithm over land. Details on the candidate aerosol models and lookup table are described below.

Finally, the uncertainties of the three aerosol parameters (τ_a, η, and ω) $\Sigma_{\hat{x}}$ were calculated from low of error propagation as follows:

$$\Sigma_{\hat{x}} = \left(\tilde{A}\Sigma^{-1}A\right)^{-1}, \qquad (9)$$

where A is the Jacobian determinant, and Σ is the error matrix of the TOA reflectances, which is calculated from Eq. (7). The three aerosol parameters (τ_a, η, and ω) where the uncertainties exceeded 1.0 were treated as invalid values.

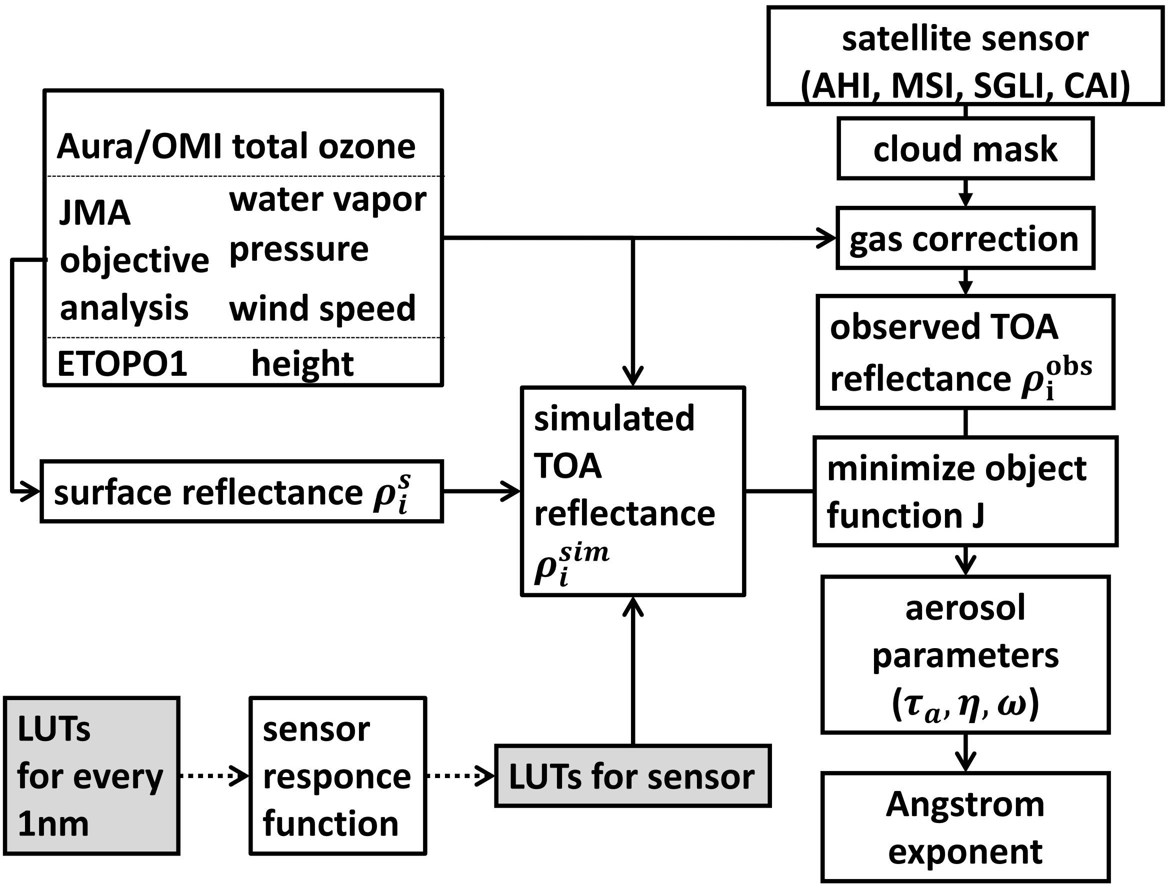

Fig. 1 Flowchart illustrating the retrieval algorithm for L2 aerosol optical properties.

4. Aerosol models

We used the common candidate aerosol models over both land and ocean to retrieve aerosols consistently over land and ocean. We assumed that the aerosol model was the external mixture of fine and coarse particles. We set the 75%H_2SO_4 model (Deepak and Gerber 1983) for the fine aerosol model but for the perturbing imaginary part of the reflective index (m_i) to represent the absorbing aerosol. For the coarse model, we set the external mixture of the Sea spray model (Deepak and Gerber 1983) with 80% relative humidity and Yellow sand model (Nakajima et al. 1989). To decrease the number of derived parameters, the imaginary part of the reflective index for fine mode varied with the external mixture ratio of Yellow sand for coarse mode so that the fine and coarse models exhibited the same ω at 500 nm.

5. Lookup Table

We used a radiative transfer code called System for the Transfer of Atmospheric Radiation developed at the University of Tokyo (STAR, Nakajima and Tanaka, 1986, 1988; Stamnes et al., 1988) for the model simulations. For rapid processing, we adopted the lookup table method (Higurashi and Nakajima, 1998). The parameters $(\rho_i^a, t_i^s, t_i^v s_i)$ in Eq. (8) were precomputed for 29 θ_0 (0.0, 2.5, 5.0…., and 70.0), 25 θ (0.0, 2.5, 5.0…., and 60.0), 37 φ (0.0, 5.0, 10.0…., and 180.0), 2 pressures (1013 and 616.6 hPa), 8 τ_a(0.0, 0.1, 0.2, 0.4, 0.8, 1.2, 1.6, and 2.0), 11 refractive indexes (external mixing ratio of dust) for fine (coarse) mode, and 4 η(0.0, 0.33, 0.66, and1.0). We calculated these parameters by the radiative transfer code for every 1 nm from 300 nm to 2500 nm. These high-resolution spectral parameters were then multiplied by the response function for SGLI.

6. Output

Output for SGLI is aerosol optical thickness, angstrom exponent, single scattering albedo, and QA flag. Table 2 shows the descriptions of the QA flag.

Table 2 SGLI QA flag

Bit Field	Flag	Result
0	Aerosol Property Algorithm	0 = Executed / 1 = Not Executed
1	Land / Water	0 = Water / 1 = Land
2	Coastal	0 = No / 1 = Yes
3	Clear / Cloud	0 = Clear / 1 = Cloudy
5, 4	AOT Confidence	00 = Very Good (suitable for validation) 01 = Good (suitable for statistics) 10 = Poor 00 = No Confidence, No Retrieval or Fill
7, 6	AE Confidence	
9, 8	SSA Confidence	
10	Sun Glint Impact	0 = No / 1 = Yes
11	Stray-light Corrected	0 = No / 1 = Yes
12	Cloud Shadow Possibility	0 = No / 1 = Yes
13	obs < rayleigh	0 = No / 1 = Yes
15, 14	Aerosol Type	TBD

References

Cox, C., and W. Munk, 1954: Statistics of the sea surface derived from sun glitter, J. Mar. Res., 13, 198–227.

Deepak, A., and H. E. Gerber 1983: Report of the experts meeting on aerosols and their climate effects, WCP-55, World Meteorological Organization, Geneva, 107 pp.

Fukuda, S., Nakajima, T., Takenaka, H., Higurashi, A., Kikuchi, N., Nakajima, T. Y., & Ishida, H.,2013: New approaches to removing cloud shadows and evaluating the 380 nm surface reflectance for improved aerosol optical thickness retrievals from the GOSAT/TANSO‐Cloud and Aerosol Imager. Journal of Geophysical Research: Atmospheres, 118(24), 13-520.

Higurashi, A., and T. Nakajima, 1999: Development of a two-channel aerosol retrieval algorithm on a global scale using NOAA AVHRR, J. Atmos. Sci., 56, 924-941.

Ishida, H., and T. Y. Nakajima, 2009: Development of an unbiased cloud detection algorithm for a spaceborne multispectral imager, J. Geophys. Res., 114, D07206, doi:10.1029/2008JD010710.

Ishida, H., T. Y. Nakajima, T. Yokota, N. Kikuchi, and H. Watanabe, 2011:

Investigation of GOSAT TANSO-CAI cloud screening ability through an inter-satellite comparison, J. Appl. Meteor. Climatol., 50, 1571–1586. doi:10.1175/2011JAMC2672.1.

MODIS Algorithm Theoretical Basis Document for Collection 005 and 051: https://modis-atmos.gsfc.nasa.gov/_docs/ATBD_MOD04_C005_rev2.pdf

Nakajima, T., and M. Tanaka, 1986: Matrix formulation for the transfer of solar radiation in a plane-parallel scattering atmosphere, J. Quant. Spectrosc. Radiat. Transfer 35, 13–21.

Nakajima, T., and M. Tanaka, 1988: Algorithms for radiative intensity calculations in moderately thick atmospheres using a truncation approximation, J. Quant. Spectrosc. Radiat. Transfer 40, 51–69.

Nakajima, T., M. Tanaka, M. Yamano, M. Shiobara, K. Arao, and Y. Nakanishi, 1989: Aerosol optical characteristics in the yellow sand events observed in May, 1982 in Nagasaki—part II model, J. Meteorol. Soc. Jpn. 67, 279–291.

Stamnes,K., S. C. Tsay, W. Wiscombe, and K. Jayaweera, 1988: Numerically stable algorithm for discrete-ordinate-method radiative transfer in multiple scattering and emitting layered media, Appl. Opt. 27, 2502–2509.